Dynamic Hard Shoulder Running Lane Control

Rodrigo Castelan Carlson, Eduardo Rosa de Lima, Eduardo Rauh Müller,
Felipe Augusto de Souza, and Konstantinos Ampountolas

***Abstract*— This work presents a novel and practical real-time switching control policy for the dynamic hard shoulder running lane control on motorways. Using the hard shoulder as a running lane in peak traffic periods increases the motorway capacity at bottlenecks, increasing throughput and avoiding the onset of congestion. The proposed policy enables a smooth switching on of the hard shoulder lane at peak periods. It is based on properties of the fundamental diagram of motorway traffic with easy and unambiguous interpretation and implementation by traffic operators. Simulation analysis on a 5 km-long motorway stretch with three lanes and one hard shoulder lane using the AIMSUN microscopic simulator is demonstrated. The results have showed that the proposed switching control improves the motorway throughput compared to rival control schemes. The proposed dynamic hard shoulder running lane control was analyzed based on the kinematic wave theory and shown to be optimal.**

I. Introduction

Motorways are uninterrupted roads operating with two or more lanes of traffic. These roads are intended to allow vehicles to travel at higher speed and flow compared to other road types such as arterials and local roads. However, traffic congestion is a common occurrence on motorways due to demand exceeding the motorway capacity and inappropriate traffic management. Allowing vehicles to use the hard shoulder lane during peak times increases motorway throughput and may mitigate congestion. However, the activation/deactivation policy must be devised so as to guarantee a smooth operation.

The purposes of hard shoulders are diverse, including emergency use and space for maintenance equipment and personnel [1]. If hard shoulders are suitable for running traffic, in some cases hard shoulders have been repurposed as managed lanes and used as special lanes, e.g., for buses, or as additional lanes of traffic to increase motorway capacity during peak hours, thus reducing traffic congestion. In some instances with too high demands the hard shoulders were made permanent running lanes [2], [3].

The fixed-time (static) operation of hard shoulders as running lanes is termed hard shoulder running (HSR). This type of operation suffers the same problems as other fixed-time traffic management strategies, see, e.g., the cases of tidal flow/reversible lanes [4] and ramp metering [5], such as early/late activation/deactivation, ageing/obsolescence of the fixed schedule/plan, and impossibility to respond to unexpected events [3]. Some of these problems also apply to manual (dynamic) operation, which, in addition, is susceptible to the subjective interpretation of the traffic conditions by the operator. The result is an inefficient operation of the traffic system.

Several works analysed practical applications of HSR [2], [6], [7], [8], [9], [10], [11], [12], [13], [14], [15], from different perspectives, such as operation efficiency, safety, environment, and pavement. However, in contrast with other traffic management measures on motorways, such as ramp metering [5] and variable speed limits [16], [17], only a few works addressed the design of real-time (dynamic) HSR strategies, see, e.g., [18], [19], [20], [21], [22], [23].

This paper aims to devise a novel and practical switching policy for efficient dynamic HSR lane control. It is based on properties of the triangular (piecewise linear) fundamental diagram and relies on real-time measurements of density only, or its proxies, such as occupancy and speed. The effectiveness of the proposed switching control is demonstrated via a microsimulation study to a hypothetical motorway stretch featuring an on-ramp merge that is subject to congestion due to high demand. Moreover the proposed policy is compared to an ad-hoc strategy proposed by [23]. Kinematic Wave Theory analysis is employed to demonstrate the optimality of the proposed strategy.

The rest of the paper is structured as follows. Section II proposes a new real-time state-feedback switching control logic for dynamic hard shoulder running lane control on motorways derived from properties of the triangular fundamental diagram. The proposed policy is analyzed based on the kinematic wave theory and shown to be optimal. An ad-hoc dynamic HSR policy is presented for comparison. The results of an analysis with microsimulation from the model of an hypothetical motorway stretch are presented in Section III. Section IV concludes the paper.

An earlier version of this work has been presented at the 37th ANPET Congresso de Pesquisa e Ensino em Transportes (National Conference in Brazil), São Paulo, Brazil, 2023.

This work was supported by The Brazilian Agency for Higher Education (CAPES), under the project PrInt CAPES-UFSC "Automation 4.0"; by the National Council for Scientific and Technological Development (CNPq) with an undergraduate student scholarship, and under grants 304555/2020-7 and 422481/2021-1; and by the U.S. Department of Energy Vehicle Technologies Office under the Systems and Modeling for Accelerated Research in Transportation Mobility Laboratory Consortium, an initiative of the Energy Efficient Mobility Systems Program.

R. C. Carlson, E. R. de Lima, and E. R. Müller are with the Department of Automation and Systems, Federal University of Santa Catarina, Florianópolis 88040-900, Brazil (e-mail: rodrigo.carlson@ufsc.br; eduardorl.ufsc@gmail.com; edurauh@gmail.com).

F. A. de Souza is with the Energy Systems, Argonne National Laboratory, Lemont, IL 60439 USA (e-mail: fdesouza@anl.gov).

K. Ampountolas is with the Automatic Control & Autonomous Systems Laboratory, Department of Mechanical Engineering, University of Thessaly, 38334 Volos, Greece (e-mail: k.ampountolas@uth.gr).

Manuscript 389 submitted to 2024 10th International Conference on Control, Decision and Information Technologies (CoDIT). Received March 5, 2024.

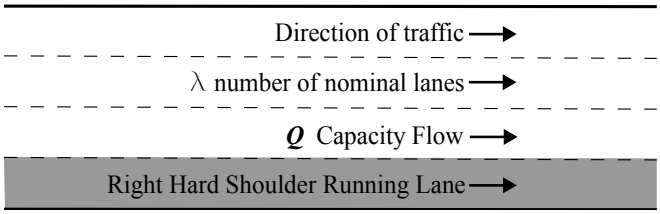

Fig. 1. An one-way motorway stretch with a shoulder adequate for HSR.

II. Dynamic Hard Shoulder Running Lane Control

This section presents the proposed state-feedback switching control policy for dynamic HSR lane control. This policy based on characteristics of the triangular fundamental diagram (FD) of uninterrupted motorway traffic.

A. HSR Switching Control

Consider a motorway stretch as shown in Fig. 1, in which the right (or left) shoulder has appropriate characteristics for use as a running lane [3]. The shoulder is shaded and permits HSR operation. This extra lane can be opened to traffic during peak periods to provide extra capacity in this direction of traffic.

We assume that, under stationary traffic conditions, the motorway stretch indicates a triangular nominal FD (nFD) as shown in Fig. 2, although the policy to be presented is valid for any strictly concave FD. This model is know to fit well with field empirical data as demonstrated in a number of practical studies, see, e.g., the work by [24], [4].

In a previous work, involving tidal flow lanes two other diagrams were proposed, the reduced FD (rFD) and the extended FD (eFD), to characterise tidal traffic flow operations [4]. In this work, there is no reduction in the number of lanes, therefore the rFD is not of interest. On the other hand, under HSR control, the eFD characterises the traffic conditions of extra capacity due to HSR activation. Schematically, the proposed control logic is illustrated with the inward arrows in Fig. 2. It relies on the gentle switching of the nFD to eFD under HSR. For instance, under stationary traffic conditions and operations, the motorway stretch shown in Fig. 1 operates under the nFD with number of lanes λ and maximum stationary flow (or capacity) Q (Fig. 2). We assume that the hard shoulder opens to provide extra capacity of traffic resulting in the motorway operating with $\lambda+1$ lanes under the eFD and capacity flow Q^{e}.

The policy to be presented next relies on the parameters of nFD and assumes the motorway operates under the eFD when the HSR is activated. The nFD and eFD can be estimated off-line provided empirical data from periods operating without HSR (nFD) and with HSR operative (eFD). We do not assume an independent fundamental diagram for the HSR. This is because the number of lanes available may have an effect on lane usage and infrastructure capacity [7], [10], [3], [25].

The developed FD-based HSR policy monitors in real-time the prevailing density ϱ and compares it with the critical density ϱ_{cr} of the nFD (Fig. 2). If overcritical conditions prevail during peak hours, i.e., its density is higher than the critical density of the nFD, then the hard shoulder lane opens to provide extra capacity to the motorway. The prevailing density ϱ continues to be monitored and compared with the critical density ϱ_{cr} of the nFD until traffic conditions are under critical and the extra capacity becomes unnecessary, then the hard shoulder lane is closed.

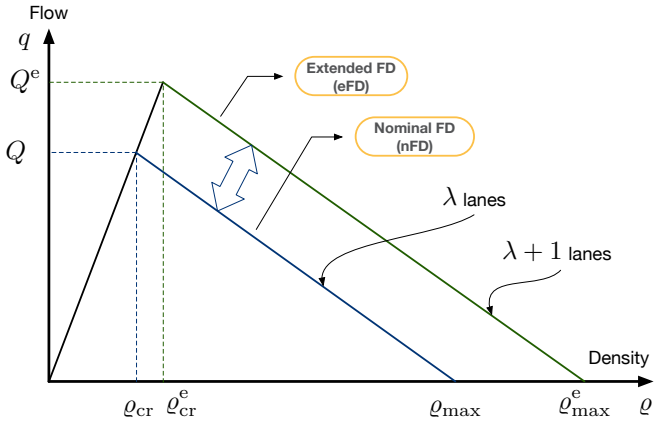

Fig. 2. Motorway nominal and extended triangular fundamental diagrams.

The FD-based HSR state-feedback switching policy corresponds to the following control law:

$$u(k+1) = \begin{cases} 1, & \text{if } u(k)=0 \text{ and } \varrho(k) > \gamma \varrho_{\mathrm{cr}}, \\ 0, & \text{if } u(k)=1 \text{ and } \varrho(k) < \gamma' \varrho_{\mathrm{cr}}, \end{cases} \tag{1}$$

with $k = 0, 1, 2, \ldots$ the discrete time index, u the state of the shoulder (opened $=1$ or closed $=0$), ϱ the density measured over all lanes, including the shoulder, and $\gamma \in [0.5, 1)$ and $\gamma' \in [0.5, 1)$, with $\gamma' < \gamma$ parameters to smooth operation against two common problems. First, an overestimation of the critical density ϱ_{cr}. The γ ensures that the HSR is activated before the demand reaches capacity Q and congestion ensues. Similar reasoning applies in the deactivation of the HSR. Second, frequent activation and deactivation of the HSR. These parameters add hysteresis to the control law and prevent excessive switching.

This control policy is executed in real-time every control period T, while ϱ is aggregated over the measurement interval T_{m}. A typical period of $T_{\mathrm{m}} = 5$–15 min can be used that sustains the motorway capacity. The control period T should be sufficiently large to avoid oscillations (e.g., frequent switching) and windup phenomena (e.g., in dead zones where control does not affect the state of the system). Note that the control may be computed more often, but be held for a minimum time after a switch occurs. Filtering can be used to smooth measurements.

The basic steps of the HSR FD-based switching policy are given in Algorithm 1. We note that:

- Lines 6 and 14–16 ensure smooth HSR operation by checking if the shoulder is clear of stalled vehicles, debris or any other feature impeding its use. We assume the status of the shoulder is constantly monitored.

Manuscript 389 submitted to 2024 10th International Conference on Control, Decision and Information Technologies (CoDIT). Received March 5, 2024.

Algorithm 1 Real-time HSR FD-Based Switching Policy

data: critical density $\varrho_{\rm cr}$ of the FD; control parameters γ and γ'; control interval T; measurement interval $T_{\rm m}$;
result: control action $u(k+1)$;
initialise: $k \leftarrow 0$; $u(k) \leftarrow 0$;
repeat at every control interval T;
  enter new measurements $\varrho(k)$ (aggregated over $T_{\rm m}$);
  if hard shoulder lane is clear **then**
    if $u(k) = 0$ and $\varrho(k) > \gamma\varrho_{\rm cr}$ **then**
      $u(k+1) \leftarrow 1$;
    else if $u(k) = 1$ **and** $\varrho(k) < \gamma'\varrho_{\rm cr}$ **then**
      $u(k+1) \leftarrow 0$;
    else
      $u(k+1) \leftarrow u(k)$;
    end if
  else
    $u(k+1) \leftarrow 0$;
  end if
  $k \leftarrow k+1$;
until control system is disabled

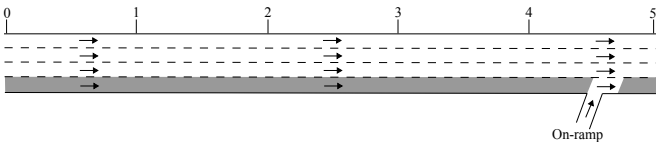

Fig. 3. Topology of the 5 km-long modelled motorway stretch with the hard shoulder shaded.

- The FD-based policy can work with proxies of density, e.g., occupancy o available from inductive-loop detectors and corresponding critical occupancy $o_{\rm cr}$, without modifications of the main logic.
- The FD-based policy is robust because it does not rely on any forecasts. It relies only on the current and observable density ϱ or proxies of the system state, the current control and on the gentle switching of the nFD to the eFD. Thus, the policy has low requirements and can be applied with limited knowledge of the environment if loop-detector data are available in real-time and a system for monitoring the status of the hard shoulder is in place.
- The proposed FD-based policy guarantees that the motorway operates in the uncongested regime provided there is no congestion mounting from downstream of the controlled motorway and the flow remains below the eFD capacity or, equivalently, $\rho_{\rm cr}^{\rm e}$ is not exceeded (see Fig. 2).

In the sequel, we will refer to this FD-based state-feedback switching HSR control logic as D-HSR.

B. Kinematic Wave Theory of HSR Lane Control

Consider the closed (no on/off-ramps) motorway stretch shown in Fig. 1 of length ℓ. Let $\varrho(x)$ be the density at location x and $F\left[\varrho(x), x\right]$ a location-dependent and concave in x fundamental diagram that provides the outflow at x when the local density is $\varrho(x)$. Assume that the downstream infrastructure (off-ramps, exit-points, etc.) has enough capacity to discharge any desired outflows. Now define as $f(x) = f(x, x+dx)/dx$ the fraction of traffic exiting per unit length of road at x. Then, the prevailing outflow in a segment $i_x \triangleq (x \mid x+dx)$ is the product of the flow $F\left[\varrho(x), x\right]$ and the fraction of vehicles $f(x)dx$ exiting in i_x. Thus the outflow is given by,

$$\mathcal{O}[\varrho(x)] = \int_0^\ell F\left[\varrho(x), x\right] f(x)\, dx. \tag{2}$$

Assume now that the motorway stretch is controlled (i.e., the HSR lane can be opened or closed by an automatic control system) in order to maintain the system in a steady state with balanced inflows and outflows. The problem of throughput maximisation now reads:

$$\max_{\varrho(x)} \quad \mathcal{O}[\varrho(x)] = \int_0^\ell F\left[\varrho(x), x\right] f(x)\, dx \tag{3}$$

$$\text{subject to:} \quad N - \int_0^\ell \varrho(x)\, dx = 0. \tag{4}$$

where N is the accumulation of vehicles within ℓ; and $\varrho(x)$ is the variable to be optimized.

This problem can be readily solved by introducing the Lagrangian associated with the constrained problem and then taking the appropriate partial derivatives equal to zero. From the first-order necessary conditions, it results that the optimal solution $\varrho^*(x)$, must satisfy:

$$f(x) w(\varrho^*(x), x) = \mu^*, \tag{5}$$

with μ^* a constant, the associated Lagrange multiplier; and, $w(\varrho, x) \triangleq \partial F(\varrho, x)/\partial\varrho$ the kinematic wave speed of the motorway stretch. The value of the Lagrange multiplier μ^* guarantees that the optimal density $\varrho^*(x)$ satisfies (4). Given that (4) is an equality constraint, μ^* can take any value in the real line, depending on N (i.e. how much crowded is the considered motorway stretch).

Assume that all traffic states observed belong to the defined FDs in Section II-A, the basic assumption of Kinematic Wave Theory (KWT) is valid. First consider the case where F is an unimodal nFD (see Fig. 4) and the HSR lane is closed (blue diagram). If μ^* is positive, then w must be positive for all x. This suggests that ϱ should be on the left branch of F for all x; i.e., the motorway stretch should be uncongested everywhere. Contrary, if μ^* is negative, then w must be negative and the infrastructure should be congested everywhere. Finally, if μ^* is zero, $|w| \approx 0$, i.e., the infrastructure should be at flow capacity everywhere ($\varrho \approx \varrho_{\rm cr}$) and system's throughput is maximised.

Consider now the case of instability, where critical traffic conditions are developed in the region B of the motorway section as shown in Fig. 4 (i.e., traffic state B is on the congested regime of the nFD). In this case ($\varrho(k) > \gamma\varrho_{\rm cr}$), the FD-based switching policy (1) opens the HSR lane for mainline traffic (i.e., $u = 1$ and the shoulder is opened). This results in motorway operating under the eFD (green diagram) with number of lanes $\lambda \leftarrow \lambda + 1$.

This switching produces the wave (B,C) as shown in Fig. 4. This is a (accelerating) rarefaction wave. The rarefaction

Manuscript 389 submitted to 2024 10th International Conference on Control, Decision and Information Technologies (CoDIT). Received March 5, 2024.

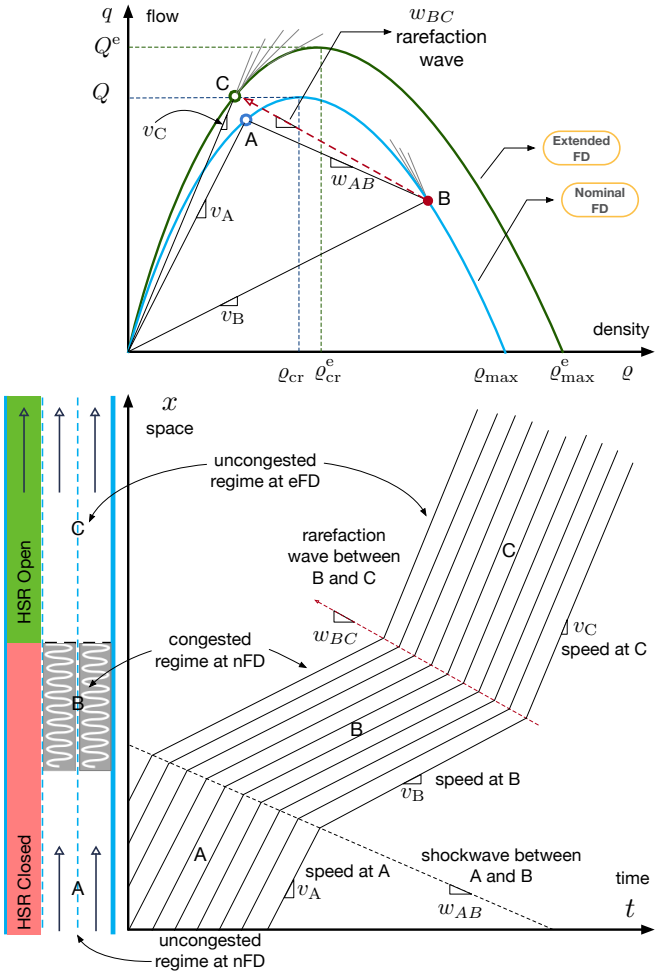

Fig. 4. HSR lane operation described by by the two FDs (nFD and eFD); Space-time diagram of various vehicle trajectories under D-HSR operation.

wave forces congested state B in the nFD to meet state C in the uncongested regime of the eFD, where (ideally) flow is increased, speed is increased while density is substantially decreased to accommodate a largest number of trips. This kind of expansion wave is referred to as a accelerating wave because the drivers experience a decrease in density (a rarefaction) as they pass through this wave while the motorway is operating under the eFD with $\lambda + 1$ lanes. It should be highlighted that according to the KWT when flow is moving from a congested state (see B in Fig. 4) to an uncongested state (see C in Fig. 4) it should follow a path on the corresponding fundamental diagram, i.e., first pass through capacity state of the nFD and then jump to the eFD. As a special property of the triangular FD $w = w_{\mathrm{f}} > 0$, and thus the switching wave (B,C) under HSR lane operation implies $\mu^* > 0$, i.e., the mainline traffic should be uncongested everywhere and should be served with the maximum $f^*(x)$ trip rate.

Moreover, Fig. 4 illustrates the spatial and temporal variation of various vehicle trajectories and the corresponding shockwaves in the (x,t)-diagram. As can be seen, initially traffic state A is uncongested and the HSR is closed. Traffic state B indicates a congested region while the HSR is still closed. It is known from the conservation of vehicles that if two regions of the space-time diagram are neighbouring they must be separated by an interface with some velocity. This is the shockwave w_{AB} created between states A and B in Fig. 4. In state B $\varrho(k) > \gamma\varrho_{\mathrm{cr}}$ holds, the FD-based switching policy (1) is activated and opens the HSR lane for mainline traffic (i.e., $u = 1$ and the shoulder is opened). This switching produces the shockwave w_{BC} as shown in Fig. 4. This results in motorway operating under the eFD with number of lanes $\lambda \leftarrow \lambda + 1$ in region C.

In summary, the proposed HSR lane control and optimality condition (5) suggest that infrastructure and density should be managed so as to maximise flow on the motorway stretch that contains the maximum number of desired destinations. Finally, it should be emphasised that maximisation of the directional exit flow is equivalent to the minimisation of the total time spent in the motorway stretch, provided control independent inflows (see e.g. [26]).

III. Application

A. Simulated Network and Demand

The AIMSUN microscopic simulator was employed to model the 5 km-long motorway stretch showed in Fig. 3. The motorway has an on-ramp merge 4.5 km downstream from the start of the stretch and three lanes plus the hard shoulder. In each lane, including the hard shoulder lane, one detector is placed in the merging area in the position where congestion is formed. The nominal speed limit on the motorway is 110 km/h and the hard shoulder lane operates with a speed limit of 70 km/h when open. We assume flashing signs on gantries above the hard shoulder lane indicate when it is open for traffic and that speed limit signs are also available. We only consider passenger cars and therefore we do not implement different rules for heavy vehicles.

Fig. 5 depicts the trapezoidal profile of the traffic demand. It emulates a peak period lasting one hour and forty minutes (100 min). The maximum demand in the mainstream is 6000 veh/h and 600 veh/h in the on-ramp, for a total maximum demand of 6600 veh/h, which exceeds the three-lane motorway capacity of $Q = 6380$ veh/h obtained from inspection of the motorway flow-density diagram (see Section III-C).

B. Simulation Setup

We study four different control policies. The first policy is a no-control scenario with the hard shoulder lane close (NC-CHS), i.e., only three lanes operating. The second policy is a no-control scenario with the hard shoulder lane open (NC-OHS), i.e., all four lanes are in operation during the whole simulation. The third policy is the A-HSR strategy by [23]. Finally, the fourth policy is the D-HSR strategy proposed in this paper in Section II-A.

For A-HSR the opening and closing threshold was chosen as $V_{\mathrm{hdr}} = 5423$ veh/h. This value was obtained by multiplying the three-lane capacity flow by $\gamma = 0.85$ used by the D-HSR strategy.

Manuscript 389 submitted to 2024 10th International Conference on Control, Decision and Information Technologies (CoDIT). Received March 5, 2024.

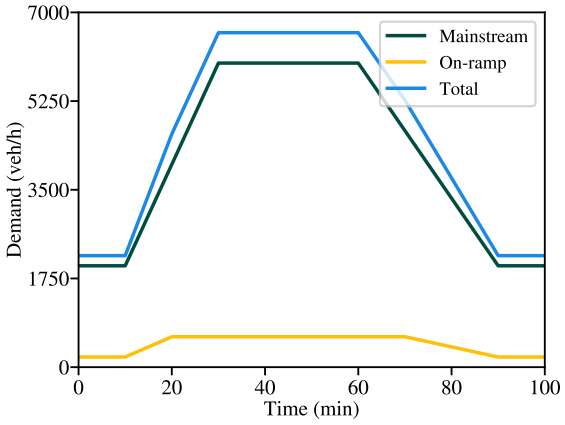

Fig. 5. Trapezoidal demand profiles for simulation of the motorway stretch.

For D-HSR the threshold parameters were set using engineering judgement, without a fine tuning or sensitivity analysis effort. The obtained values are $\gamma = 0.85$, as also used in the A-HSR, and $\gamma' = 0.60$. This creates a hysteresis band between 60 and 85% of the three-lane critical density that avoids undesired frequent switching of the hard shoulder lane. The three-lane critical density was obtained from inspection of the flow-density diagram of the NC-CHS (see Section III-C) as $\varrho_{\mathrm{cr}} = 83$ veh/km.

The HSR control interval in both cases is $T = 1$ min, with a minimum time interval of 15 min between consecutive switchings. In the case of A-HSR, the VSL control period is of 5 min as proposed by [23]. The measurements used for control are obtained from moving averages of one-minute interval measurements taken for the last $T_{\mathrm{m}} = 5$ min.

Ten replications with different seeds were run for each control policy and were sufficient to obtain mean estimates of the total time spent (TTS) with 95% confidence of an error below 10% [27].

C. Results

The average TTS of the ten replications of each policy and their relative improvement over the NC-CHS are shown in Table I. The first five minutes of the simulation were considered as a warm-up period to fill the network and were discarded for the computation of TTS. The improvement of the control scenarios compared to the scenario without the use of the hard shoulder lane is expected. The important results stems from the temporary use of the shoulder that provides extra capacity only when needed, preserving the hard shoulder lane pavement and road safety [7]. The NC-OHS serves as an upper bound of possible improvement. The verification of the results through two-tailed t-tests with 95% confidence level showed that the difference of the TTS averages between all policies is statistically significant, except between NC-OHS and D-HSR.

Fig. 6 presents the control actions along with smoothed flow, density, speed, and measured flow-density diagrams at the merge area for all scenarios. A replication with TTS close to the averages was used in these figures. In the NC-CHS

TABLE I

TOTAL TIME SPENT (TTS) FOR ALL SIMULATED CONTROL POLICIES

Scenario	TTS (veh·h)	Improvement (%)
NC-CHS	414.5	-
NC-OHS	216.2	47.8
A-HSR	221.4	46.6
D-HSR	217.7	47.5

policy, we see the flow increasing up to the three-lane (nFD) capacity flow of $Q = 6380$ veh/h after 35 min of simulation. This corresponds to the time the density at the merge area exceeded $\rho_{\mathrm{cr}} = 83$ veh/km and a sharp decrease in speed occurs. The capacity flow and critical density can be verified on the flow-density diagram, which resembles a triangular fundamental diagram.

The NC-OHS policy shows a similar behaviour as the NC-CHS up to 35 min. However, since the hard shoulder lane is open, the capacity flow Q^{e} and the critical density $\rho_{\mathrm{cr}}^{\mathrm{e}}$ are not reached. Thus, the flow remains at around the maximum demand flow of 6600 veh/h. The density barely reaches the three-lane motorway critical density and the speed remains high. Because there is no congestion, we see only the left branch of the flow-density diagram and, because there are four lanes in total, there are points at higher values than in the case of NC-CHS.

The A-HSR and D-HSR policies show a behaviour similar to the NC-OHS policy. As expected from the TTS results, the timely activation of the shoulder lane enables a good performance of the traffic system comparable to the one by the NC-OHS. In the A-HSR the activation of the hard shoulder lane is seen to occur at around 30 min when the flow exceeds the value of V_{hdr} and the deactivation occurs some 40 min later when the threshold is crossed in the opposite direction. We see that the A-HSR speed limit is reduced from 110 km/h to 100 km/h a few minutes before HSR action because the per lane flow exceeded 1650 veh/h and is increased back to 110 km/h a few minutes later. This occurs because, being the logic based on per lane flow measurements, the addition of one lane takes the per lane flow to a value below 1650 veh/h. Note that the reversed behaviour occurs at around 70 min due to the deactivation of the HSR. Between 30 and 70 min we see a few changes of speed limits. This happens because the peak flow is 6600 veh/h, corresponding to 4×1650 veh/h/lane. Thus, the variations in the measured flow, despite the use of a smoothing filter, cause frequent changes of speed limit. The flow-density diagram is not distinguishable from the NC-OHS case.

In the D-HSR the activation of the hard shoulder lane occurs slightly later than the A-HSR, when the density exceeds the value of $\gamma\rho_{\mathrm{cr}}$. The deactivation occurs some 10 min after the A-HSR when the threshold given by $\gamma'\rho_{\mathrm{cr}}$ is crossed. Slightly less variations are observed in flow, density and speed in the peak-period than A-HSR, following closely the NC-OHS, except for some 10 min around the time of the HSR activation. The flow-density diagram is not

Manuscript 389 submitted to 2024 10th International Conference on Control, Decision and Information Technologies (CoDIT). Received March 5, 2024.

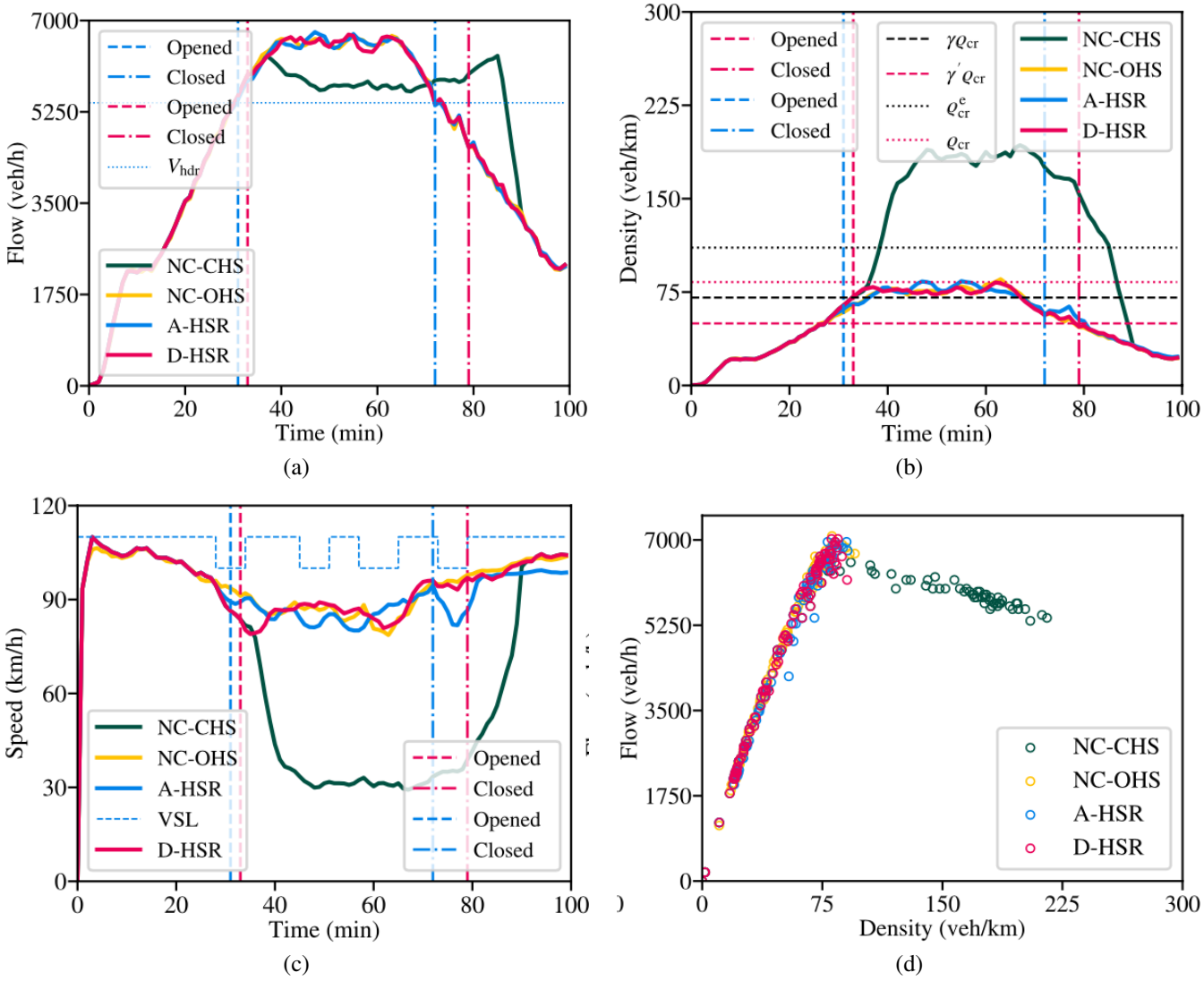

Fig. 6. Control actions, flow, density, speed, and flow-density diagrams at the merge area for all scenarios

distinguishable from the NC-OHS or A-HSR cases.

Fig. 7 shows time-space diagrams of density for the four policies using the same replication as in Fig. 6. The density in this case is presented per lane ($\rho_{cr} = 27.7$ veh/km/lane). In accordance with the density plot in Fig. 6, we see that the congestion in the NC-CHS starts forming at the bottleneck at around 35 min. The congestion is sustained for around 50 min with a maximum extension of 3.5 km. The space-time diagrams for NC-OHS, A-HSR, and D-HSR show under critical densities corresponding to free flowing traffic.

IV. Conclusions

The state feedback D-HSR policy for the efficient operation of HSR lanes on motorways was presented. Its simplicity stems from the properties of the fundamental diagram of motorway traffic that requires only density measurements and offline estimates of the motorway critical density. The effectiveness of the proposed D-HSR policy was demonstrated via a microsimulation study, analyzed based on the kinematic wave theory, and shown to be optimal.

The improvement of the traffic system performance and increased bottleneck throughput by the addition of a running lane is trivial. In the HSR problem, the matter is when the hard shoulder lane should be activated to guarantee a safe and optimal use of the motorway infrastructure. This is important because, often, the hard shoulder pavement is not as robust as the main lanes. In addition, the hard shoulder may have an important effect on traffic safety [7], including being an escape area for stalled vehicles, even if safety bay areas are available on the road side. On the other hand, there are incurred costs for deployment and operation of the real-time operation of the system.

The proposed switching policy can be integrated with other strategies, such as ramp metering [5], variable speed limits [28], and tidal flow control [4]. The calibration and sensitivity of threshold parameters in D-HSR and a study case with a model of a real motorway are left for future work.

Manuscript 389 submitted to 2024 10th International Conference on Control, Decision and Information Technologies (CoDIT). Received March 5, 2024.

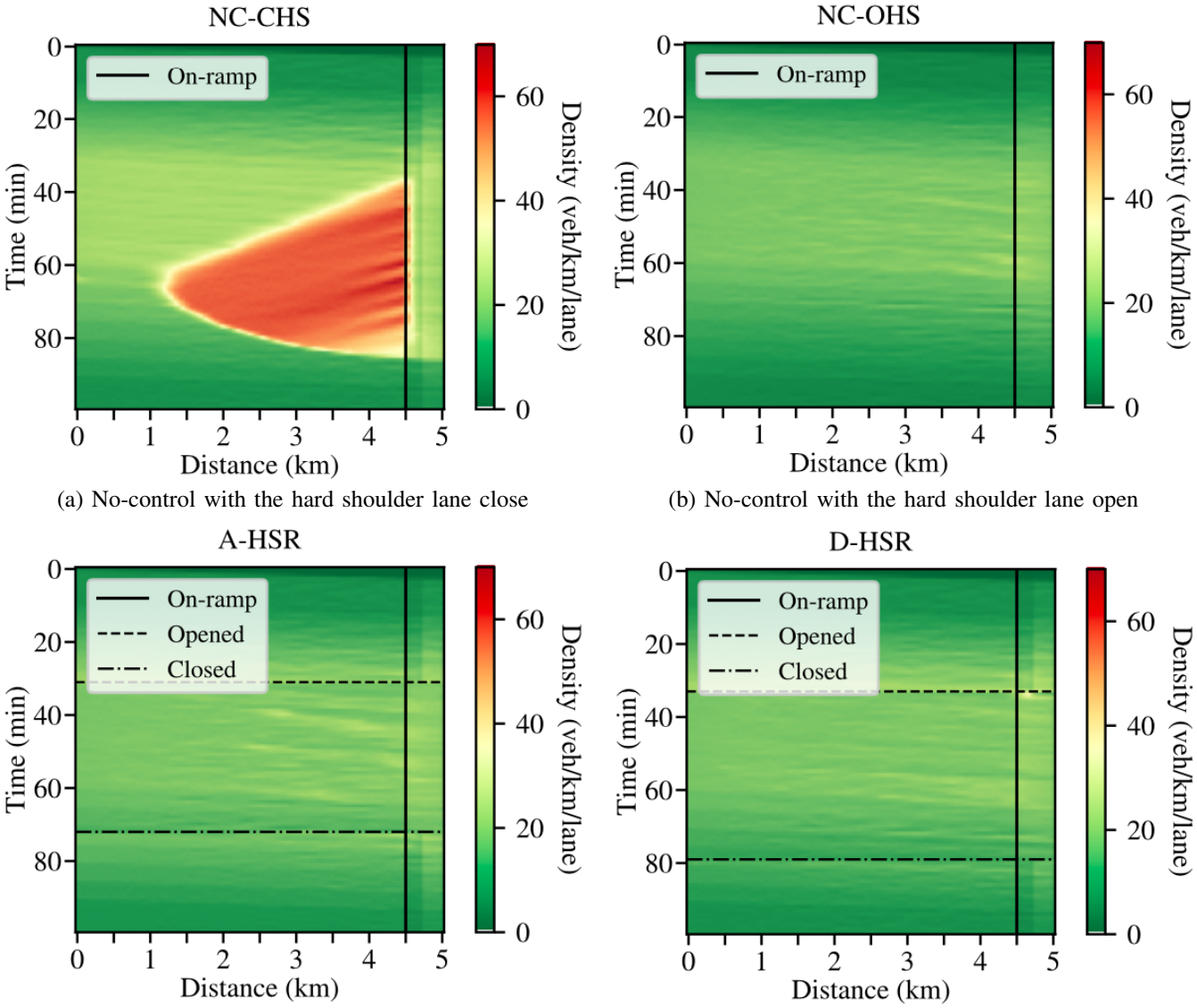

(a) No-control with the hard shoulder lane close

(b) No-control with the hard shoulder lane open

(c) Ad-hoc HSR policy by [23]

(d) FD-based switching control of HSR (D-HSR)

Fig. 7. Time-space diagrams of density for all control policies.

REFERENCES

[1] R. P. Roess, E. S. Prassas, and W. R. McShane, *Traffic Engineering*, 4th ed. Upper Saddle River, NJ: Pearson, 2011.

[2] M. Aron, S. Cohen, and R. Seidowsky, "Two french hard-shoulder running operations: Some comments on effectiveness and safety," in *13th IEEE Conference on Intelligent Transportation Systems*, 2010, pp. 230–236.

[3] P. Jenior, R. Dowling, B. Nevers, and L. Neudorff, "Use of freeway shoulders for travel – Guide for planning, evaluating, and designing part-time shoulder use as a traffic management strategy," FHWA, Technical Informational Report FHWA-HOP-15-023, 2016.

[4] K. Ampountolas, J. A. dos Santos, and R. C. Carlson, "Motorway tidal flow lane control," *IEEE Transactions on Intelligent Transportation Systems*, vol. 21, no. 4, pp. 1687–1696, 2020.

[5] M. Papageorgiou and A. Kotsialos, "Freeway ramp metering: an overview," *IEEE Transactions on Intelligent Transportation Systems*, vol. 3, no. 4, pp. 271–281, 2002.

[6] H. Zheng, E. Nava, and Y.-C. Chiu, "Evaluating active traffic and demand management strategies for congested tourism traffic corridor," in *14th International IEEE Conference on Intelligent Transportation Systems*, 2011, pp. 2015–2020.

[7] J. Geistefeldt, "Operational experience with temporary hard shoulder running in germany," *Transportation Research Record*, vol. 2278, no. 1, pp. 67–73, 2012.

[8] R. Vadde, D. Sun, J. O. Sai, M. A. Faruqi, and P. T. Leelani, "A simulation study of using active traffic management strategies on congested freeways," *Journal of Modern Transportation*, vol. 20, no. 3, pp. 178–184, 2012.

[9] M. Aron, R. Seidowsky, and S. Cohen, "Safety impact of using the hard shoulder during congested traffic. The case of a managed lane operation on a French urban motorway," *Transportation Research Part C: Emerging Technologies*, vol. 28, pp. 168–180, 2013.

[10] S. Samoili, D. Efthymiou, C. Antoniou, and A.-G. Dumont, "Investigation of lane flow distribution on hard shoulder running freeways," *Transportation Research Record*, vol. 2396, no. 1, pp. 133–142, 2013.

[11] H. Haj-Salem, N. Farhi, and J.-P. Lebacque, "Combining ramp metering and hard shoulder strategies: Field evaluation results on the ile the france motorway network," *Transportation Research Procedia*, vol. 3, pp. 1002–1010, 2014.

[12] S. Coffey and S. Park, "State of the non-operations based research of hard shoulder running," *Procedia Engineering*, vol. 145, pp. 693–698, 2016.

[13] J. Choi, R. Tay, S. Kim, S. Jeong, J. Kim, and T.-Y. Heo, "Safety

effects of freeway hard shoulder running," *Applied Sciences*, vol. 9, no. 17, p. 3614, 2019.
[14] H. Waleczek and J. Geistefeldt, "Long-term safety analysis of hard shoulder running on freeways in germany," *Transportation Research Record*, vol. 2675, no. 8, pp. 345–354, 2021.
[15] F. Yang, F. Wang, F. Ding, H. Tan, and B. Ran, "Identify optimal traffic condition and speed limit for hard shoulder running strategy," *Sustainability*, vol. 13, no. 4, p. 1822, 2021.
[16] X.-Y. Lu and S. E. Shladover, "Review of variable speed limits and advisories: Theory, algorithms, and practice," *Transportation Research Record*, vol. 2423, no. 1, pp. 15–23, 2014.
[17] B. Khondaker and L. Kattan, "Variable speed limit: An overview," *Transportation Letters*, vol. 7, no. 5, 2015.
[18] Y. Li, A. H. F. Chow, and D. L. Cassel, "Optimal control of motorways by ramp metering, variable speed limits, and hard-shoulder running," *Transportation Research Record*, vol. 2470, no. 1, pp. 122–130, 2014.
[19] R. Li, Z. Ye, B. Li, and X. Zhan, "Simulation of hard shoulder running combined with queue warning during traffic accident with CTM model," *IET Intelligent Transport Systems*, vol. 11, no. 9, pp. 553–560, 2017.
[20] W. Zhou, M. Yang, M. Lee, and L. Zhang, "Q-learning-based coordinated variable speed limit and hard shoulder running control strategy to reduce travel time at freeway corridor," *Transportation Research Record*, vol. 2674, no. 11, pp. 915–925, 2020.
[21] F. F. Hussein, B. Naik, and G. A. Süer, "Development of hybrid hard shoulder running operation system for active traffic management," in *International Conference on Transportation and Development 2020*. Seattle, Washington: American Society of Civil Engineers, 2020, pp. 194–205.
[22] K. Arora and L. Kattan, "Operational and safety impacts of integrated variable speed limit with dynamic hard shoulder running," *Journal of Intelligent Transportation Systems*, pp. 1–30, 2022.
[23] D. Li and J. Lasenby, "Mitigating urban motorway congestion and emissions via active traffic management," *Research in Transportation Business & Management*, vol. 48, p. 100789, 2022.
[24] J. H. Banks, "Review of empirical research on congested freeway flow," *Transportation Research Record*, vol. 1802, no. 1, pp. 225–232, 2002.
[25] M. Guerrieri and R. Mauro, "Capacity and safety analysis of hard-shoulder running (HSR): A motorway case study," *Transportation Research Part A: Policy and Practice*, vol. 92, pp. 162–183, 2016.
[26] M. Papageorgiou and A. Kotsialos, "Freeway ramp metering: An overview," *IEEE Trans. Intell. Transport. Syst.*, vol. 3, no. 4, pp. 271–281, 2002.
[27] A. M. Law, *Simulation modeling and analysis*, 5th ed. Dubuque: McGraw-Hill Education, 2013.
[28] R. C. Carlson, I. Papamichail, M. Papageorgiou, and A. Messmer, "Optimal motorway traffic flow control involving variable speed limits and ramp metering," *Transportation Science*, vol. 44, no. 2, pp. 238–253, May 2010.